Proc. Natl. Acad. Sci. USA
Vol. 90, pp. 3583–3587, April 1993
Biophysics

Structure-based inhibitor design by using protein models for the development of antiparasitic agents

CHRISTINE S. RING*, EUGENE SUN†, JAMES H. MCKERROW*†‡, GARSON K. LEE†, PHILIP J. ROSENTHAL†, IRWIN D. KUNTZ*§, AND FRED E. COHEN*†§¶

Departments of *Pharmaceutical Chemistry, §Biochemistry and Biophysics, ‡Pathology, and †Medicine, University of California, San Francisco, CA 94143-0446

Communicated by Seymour J. Klebanoff, December 24, 1992 (received for review October 30, 1992)

ABSTRACT **The lack of an experimentally determined structure of a target protein frequently limits the application of structure-based drug design methods. In an effort to overcome this limitation, we have investigated the use of computer model-built structures for the identification of previously unknown inhibitors of enzymes from two major protease families, serine and cysteine proteases. We have successfully used our model-built structures to identify computationally and to confirm experimentally the activity of nonpeptidic inhibitors directed against important enzymes in the schistosome [2-(4-methoxybenzoyl)-1-naphthoic acid, K_I = 3 μM] and malaria {oxalic bis[(2-hydroxy-1-naphthylmethylene)hydrazide], IC_{50} = 6 μM} parasite life cycles.**

Proteases are involved in many important biological processes including protein turnover, blood coagulation, complement activation (1), hormone processing (2), and cancer cell invasion (3). Thus, they are frequently chosen as targets for drug design and discovery. Noteworthy examples include the design of angiotensin-converting enzyme inhibitors for the treatment of hypertension (4) and programs to develop human immunodeficiency virus protease inhibitors to block proliferation of the AIDS virus (5). The critical role proteases play in the life cycle of parasitic organisms also makes them attractive drug-design targets for these infectious diseases (6).

In the most simple terms, structure-based drug design methods identify favorable and unfavorable interactions between a potential inhibitor and target receptor and maximize the beneficial interactions to increase binding affinity. Obtaining an accurate structure for the receptor or ligand–receptor complex is a logical step in this process. X-ray crystallography continues to be the source of high-resolution information about protein structures. However, considerable delays often exist between determining the sequence of a protein and solving its structure. Difficulties in protein expression and more commonly in protein crystallization can delay x-ray structure determination.

Currently, no general method exists for predicting tertiary structure from amino acid sequences. However, when a protein target is homologous to another protein or group of proteins of known structure, a sensible model structure can be proposed. Recent comparisons between model and crystal structures permit an assessment of the overall accuracy expected from homology model-built structures (7–9). For a sequence that is 80% identical to a protein of known structure, the expected rms deviation of the core residues is ≈0.6 Å (10). The expected rms deviation increases to 1.8 Å when the sequences are only 20% identical. However, model-built structures could still be useful in finding previously unknown lead compounds despite the uncertainties in the lower part of this range if the errors cluster far away from the enzyme active site.

The proteases targeted for inhibitor design in this study are important in establishing schistosome infection or necessary for the maintenance of malarial infection. Schistosomiasis is a snail-borne disease that is contracted by individuals who come into contact with the parasites in infested waters. Infectious larvae (cercariae) secrete an elastase to invade the skin of the human host and initiate infection. Once in the circulatory system, the schistosomes mature and reproduce. Thousands of eggs become trapped in the portal circulation of the liver, and the host immune response leads to portal hypertension. The protease that is implicated in skin penetration has been purified and characterized, and preliminary studies suggest that cutaneous application of an inhibitor of the cercarial elastase might prevent infection (11).

The increased incidence of drug-resistant strains of malaria (especially *Plasmodium falciparum*) necessitates the search for new therapies. Malaria infection includes an erythrocytic phase that is responsible for all the clinical manifestations of the disease (12). During this phase, erythrocytic trophozoites degrade hemoglobin as a principal source of amino acids. Rosenthal and coworkers (13, 14) have identified a critical cysteine protease that appears to be involved in the degradation of hemoglobin, the parasites' primary source of amino acids. Blocking this enzyme with cysteine protease inhibitors [L-*trans*-epoxysuccinylleucylamido-(4-guanidino)butane (E64), benzyloxycarbonyl-Phe-Arg-fluoromethyl ketone] in culture arrests further growth and development (15). Thus, this enzyme is a promising target for new modes of antimalarial chemotherapy.

METHODS

Model Construction. Three-dimensional models of the structures of cercarial elastase and trophozoite cysteine protease were built following the approach of Blundell and coworkers (16, 17). Seven mammalian serine proteases, bovine chymotrypsin (18), porcine pancreatic elastase (19), rat mast cell protease (20), human neutrophil elastase (21), rat tonin (22), porcine kallikrein (23), and bovine trypsin (24), were used to derive a structural alignment for cercarial elastase (25). Papain (26) and actinidin (27) were used for trophozoite cysteine protease. The conformations of side chains were retained when possible, and the statistically most likely rotamer was selected when no conformational information was available (17). Loops were placed by using a combination of the loop dictionary and key residue approaches (28, 29). The resulting models were refined by

The publication costs of this article were defrayed in part by page charge payment. This article must therefore be hereby marked "*advertisement*" in accordance with 18 U.S.C. §1734 solely to indicate this fact.

Abbreviations: P1 and S1, amino acid residues on the acyl side of the scissile bond are denoted P1, P2, . . . P*n*, and those on the leaving group side of the scissile bond are denoted as P1′, P2′, . . . P*n*′; corresponding binding sites on the enzyme are S1, S2, . . . S*n* and S1′, S2′, . . . S*n*′.

¶To whom reprint requests should be addressed.

energy minimization with the AMBER potential function (30). Models were validated with several computational strategies, including QPACK to probe side-chain volume (31), the profile method of Luthy *et al.* (32), a Ramachandran map analysis of backbone geometry, and solvent-accessibility calculations (33).

Screening the Fine Chemicals Directory Using DOCK3.0. The two protease model structures were used as receptors for ligand docking. DOCK3.0 is an automatic method to screen small-molecule data bases for ligands that could bind to a given receptor (34). DOCK3.0 characterizes the grooves and invaginations of the active site with sets of overlapping spheres. The generated sphere centers constitute an irregular grid that can be matched with the atom centers of a potential ligand. The quality of fit of a ligand to the binding site is judged either by shape complementarity or by a simplified molecular mechanics force-field energy (estimated interaction energy).

DOCK 3.0 was used to search the Fine Chemicals Directory (Molecular Design Limited, San Leandro, CA) of 55,313 commercially available small molecules. The structures of the small molecules were obtained computationally by using a heuristic algorithm, CONCORD, developed by R. Pearlman at the University of Texas. CONCORD-generated structures are estimated to be ≈90% in agreement with those structures optimized by molecular mechanics calculations (35). The Fine Chemicals Directory was chosen over the Cambridge Structural Database of experimentally determined structures because of the ease with which interesting compounds could be obtained.

In a typical DOCK search, the top-scoring 100–200 molecules are examined with 10–50 of these selected for experimental testing (36). Because model protein structures were used instead of crystallographically determined structures, an arbitrarily large number of small molecules were saved. For each enzyme system, the 2200 molecules with the best shape-complementarity scores and the 2200 with the best force-field scores were saved. The resulting 8800 compounds were visually screened in the context of the active site by using the molecular display software MIDASPLUS (37).

Because of the uncertainties inherent in model-built structures, the scores generated by DOCK3.0 did not influence the visual screening process. Instead, compounds were judged solely on how they might interact with the active site in the putative ligand–receptor complex. In an effort to be self-consistent, the resulting 8800 compounds were screened three times. No compounds were selected during the first screening in an attempt to get acquainted with the systems. During the second and third passes, compounds that filled the site and had potential hydrogen-bonding and electrostatic interactions were selected for further inspection. Only compounds that were chosen on both the second and third screenings were considered further. From this list, an effort was made to choose compounds that were chemically diverse and that appeared to interact with the receptor in different ways. Fifty-two compounds were ultimately chosen for testing against the cercarial elastase, and 31 compounds were chosen for testing against the trophozoite cysteine protease. This screening process took ≈1 week of effort. As the enzyme-active sites became more familiar with each successive pass, the time needed to examine the ligand–receptor complex shortened.

Of the 52 compounds selected for the cercarial elastase, 33 compounds were from the force-field list, 10 compounds were from the shape list, and 9 compounds appeared on both lists. Of the 31 compounds selected for the malarial protease, 20 compounds were from the shape list, and 11 compounds were from the force-field list. These compounds were ranked as high as 4th and as low as 1939th (out of 2200) by the scores generated by DOCK3.0.

K_i Determination for the Inhibitors Against Cercarial Elastase, Chymotrypsin, and Elastase. Cercarial elastase was purified as described (38). Initial reaction velocities were determined at room temperature for each enzyme by using tetrapeptide thiobenzyl ester substrates in the presence of 20 μM 4,4'-dithiopyridine and following the absorbance at 324 nM for 1 min after enzyme addition (39). Enzyme concentrations were determined by active-site titration with chloromethyl ketone inhibitors, and used at 1/100th of the lowest substrate concentration. The reaction buffer was 100 mM glycine·NaOH, pH 9.0/2 mM $CaCl_2$. The specific substrates used were *N*-succinylalanylalanylprolylphenylalanyl thiobenzyl ester for cercarial elastase and chymotrypsin, and *N*-succinylalanylalanylalanylprolylalanyl thiobenzyl ester for pancreatic elastase at concentrations from 25 to 500 μM. Inhibitors were prepared as 100 mM stock solutions in dimethyl sulfoxide and used at concentrations from 0 to 100 μM. Reaction velocities were determined in triplicate for each point and plotted by using the method of Dixon. Data were also plotted using the Hanes transformation of the Michaelis–Menten equation to ascertain the competitive nature of inhibition. K_i was determined directly from the Dixon plot (40) and confirmed by replots of K_m^{app}/V^{app} from the Hanes plot (41).

The Trophozoite Cysteine Protease Inhibitor Studies. Enzyme activity was measured with the fluorogenic substrate benzyloxycarbonyl-Phe-Arg-(7-amino-4-methylcoumarin) as described (15). Trophozoite extracts were incubated with reaction buffer (in 0.1 M sodium acetate/10 mM dithiothreitol, pH 5.5) and an appropriate concentration of inhibitor for 30 min at room temperature. Benzyloxycarbonyl-Phe-Arg-(7-amino-4-methylcoumarin) (50 μM final concentration) was then added, and fluorescence (380 nM excitation, 460 nM absorbance) was measured continuously over 30 sec. The slope of fluorescence over time for each inhibitor concentration was compared with that of controls in multiple assays,

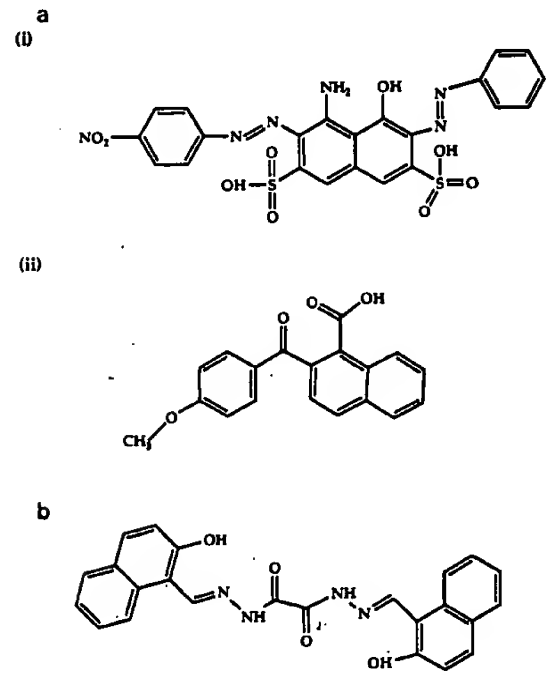

FIG. 1. (*a*) (*i*) Naphthol blue-black. (*ii*) 2-(4-Methoxybenzoyl)-1-naphthoic acid. (*b*) Oxalic bis[(2-hydroxy-1-naphthylmethylene)hydrazide].

Table 1. K_i values for compounds that inhibit cercarial elastase

Inhibitor	Cercarial elastase, K_i	Chymotrypsin, K_i	Pancreatic elastase, K_i
Naphthol blue-black	6 μM	6 μM	200 μM
2-(4-Methoxybenzoyl)-1-naphthoic acid	3 μM	30 μM	146 μM

and the IC_{50} was determined from plots of percent control activity over inhibitor concentration.

Effect of Oxalic Bis[(2-hydroxy-1-naphthylmethylene)hydrazide] on [^{3}H]Hypoxanthine Uptake as a Measure of Parasite Metabolism. [^{3}H]Hypoxanthine uptake was measured based on a modification of the method of Desjardins *et al.* (42). Microwell cultures of synchronized ring stage *P. falciparum* parasites were incubated with inhibitor in dimethyl sulfoxide (10% final concentration) for 4 hr. [^{3}H]Hypoxanthine was added (1 μCi per microwell culture; 1 Ci = 37 GBq), and the cultures were maintained for an additional 36 hr. The cells were then harvested and deposited onto glass-fiber filters that were washed and dried with ethanol. [^{3}H]Hypoxanthine uptake was quantitated by scintillation counting. The uptake at each inhibitor concentration was compared with that of controls, and the IC_{50} value was determined from plots of percent control uptake over inhibitor concentration.

RESULTS AND DISCUSSION

Nonpeptidic inhibitors were identified for both the cercarial elastase and the malarial cysteine protease. Approximately 10% of the compounds tested, 5 of 52 for the cercarial elastase and 4 of 31 for the malarial protease, displayed activity against the enzymes at concentrations <100 μM. Among these, three compounds were inhibitors at concentrations <10 μM (Fig. 1). 2-(4-Methoxybenzoyl)-1-naphthoic acid and naphthol blue-black inhibited the cercarial elastase with K_i values of 3 and 6 μM, respectively (Table 1 and Fig. 2). These two compounds also displayed specificity for the cercarial elastase, as evidenced by the generally higher K_i values against chymotrypsin and pancreatic elastase (Table 1). Because the S1 specificity pocket of cercarial elastase is more similar to chymotrypsin than to pancreatic elastase, it is not surprising that both 2-(4-methoxybenzoyl)-1-naphthoic acid and naphthol blue-black are also good inhibitors of chymotrypsin. (Note that the amino acid residues on the acyl side of the scissile bond are denoted P1, P2, . . . P*n*, and those on the leaving group side of the scissile bond are denoted as P1', P2', . . . P*n*'. The corresponding binding sites on the enzyme are S1, S2, . . . S*n* and S1', S2', . . . S*n*'.) Presumably, the application of standard medicinal chemistry strategies to these lead compounds will yield more potent and selective inhibitors of the schistosome enzyme. Topical application of peptide-based inhibitors has already been demonstrated to block parasite migration through the skin (11).

Oxalic bis[(2-hydroxy-1-naphthylmethylene)hydrazide] inhibited the trophozoite cysteine protease with an IC_{50} of 6 μM (Fig. 3*a*). When tested against cultured *P. falciparum*, this compound also inhibited the incorporation of hypoxanthine, a standard marker of parasite metabolism, at approximately the same concentration (Fig. 3*b*). Because this compound can inhibit the protease and the parasite, efforts are underway to synthesize analogs of oxalic bis[(2-hydroxy-1-naphthylmethylene)hydrazide] and examine their therapeutic potential.

The visual screening process was reexamined for the most active compounds in an attempt to find the relevant factors responsible for their selection. An interesting dichotomy was observed in the DOCK shape-based and force-field scores. All

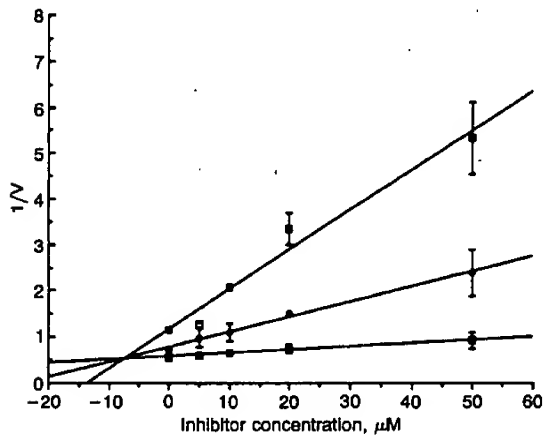

FIG. 2. Representative K_i determination using the Dixon plot. In this example, the K_i is determined for naphthol blue-black against cercarial elastase. Each point was determined in triplicate. Each line represents a different substrate concentration (■, 500 μM; ◆, 200 μM; □, 50 μM). Some error bars are too small to be graphed on this plot. V, velocity.

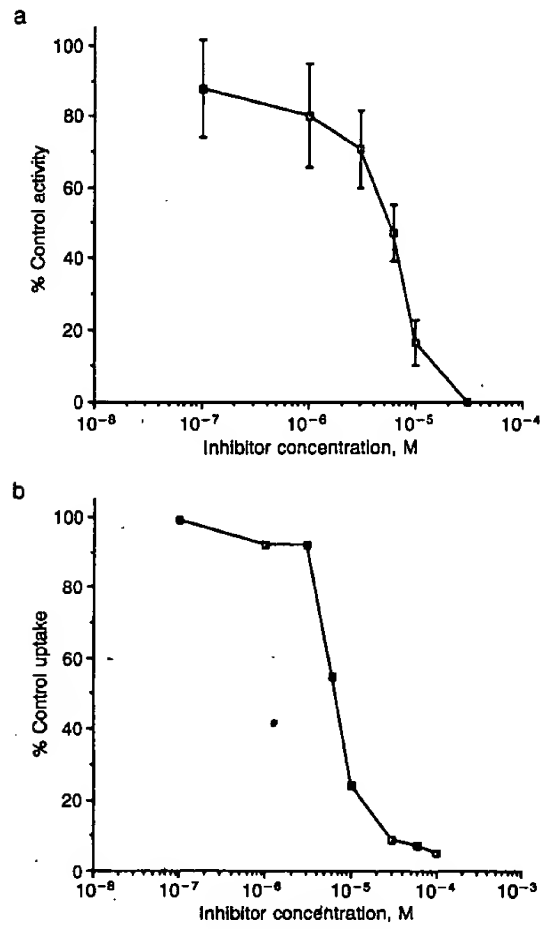

FIG. 3. (*a*) IC_{50} curve for oxalic bis[(2-hydroxy-1-naphthylmethylene)hydrazide] against malarial cysteine protease. The points are the means of eight assays, and the error bars are the SDs of the samples. (*b*) Inhibition of parasite uptake of [^{3}H]hypoxanthine by oxalic bis[(2-hydroxy-1-naphthylmethylene)hydrazide].

but one of the five inhibitors of the cercarial elastase were members of the force list with the following rankings: 85th, 2-(4-methoxybenzoyl)-1-naphthoic acid; 122nd, plasmocorinth B; 627th, naphthol blue-black; and 918th, α-phenethylphthalamic acid. The fifth compound, 9-fluorenone-4-carboxylic acid, appeared on both lists, ranking 561st on the force-field list and 1783rd on the shape-based list. The two best cercarial elastase inhibitors, 2-(4-methoxybenzoyl)-1-naphthoic acid and naphthol blue-black, ranked 85th and 627th, respectively, on the force-field list. By contrast, all four of the malarial protease inhibitors were members of the shape-based list, ranking as follows: 7th, 3,3′-diethyloxatricarbocyanine iodide; 13th, oxalic bis[(2-hydroxy-1-naphthylmethylene)hydrazide]; 793rd, cephaloglycin; and 1193rd, 1-(2-methoxyphenyl)-6-(4-trifluoromethylphenyl)-5-thiobiurea. The best inhibitor, oxalic bis[(2-hydroxy-1-naphthylmethylene)hydrazide], ranked 13th. These results may reflect the environmental differences in the active site. The active site of the malarial protease consists of a large hydrophobic cleft. Because of the absence of charged residues in the vicinity of the putative binding site, the shape-based scores for hydrophobic ligands that fill the site may adequately estimate the enthalpy of interaction between ligand and receptor. By contrast, the active site of the cercarial elastase contains both a hydrophobic S1 pocket and charged amino acids in the vicinity of the active site. Consequently, the force-field scores, which include both van der Waals and electrostatic components, better estimate the interaction energy of the ligands with the active site of the cercarial elastase.

The DOCK-generated enzyme–inhibitor complex structures for naphthol blue-black and oxalic bis[(2-hydroxy-1-naphthylmethylene)hydrazide] are shown in Fig. 4. Naphthol blue-black fits into the groove defined by the S1, S2, and S3 subsites of the cercarial elastase. In the model complex, ligand binding is stabilized by the interaction of a phenyl group with the hydrophobic S1 pocket. The sulfonic acid groups could hydrogen-bond with arginines in a nearby loop or possibly with the solvent. Similarly, oxalic bis[(2-hydroxy-1-naphthylmethylene)hydrazide] interacts with S2 and S1′ sites of the malarial protease. The hydrophobic specificity site, S2, is filled by a naphthol group. The other naphthol group participates in a stacking interaction with the indole ring of Trp-177 at the S1′ site. In addition, each hydroxyl group on the naphthol rings appears to hydrogen-bond to Ser-160 at S2 and Gln-19 at S1′. These complexes are useful starting points for modeling ligand–receptor interactions, but other possible binding modes should also be considered.

At micromolar concentrations, it is likely that the inhibitors will have multiple modes of binding to the enzyme. Because these different binding modes are approximately isoenergetic, discriminating among the plausible alternatives with current scoring functions is difficult. Assumptions, such as rigid ligands and rigid receptors, are necessary for computational tractability but are also presumably responsible for the loss of resolution in these scores. The x-ray structures of thymidylate synthase complexed with two different inhibitors that were

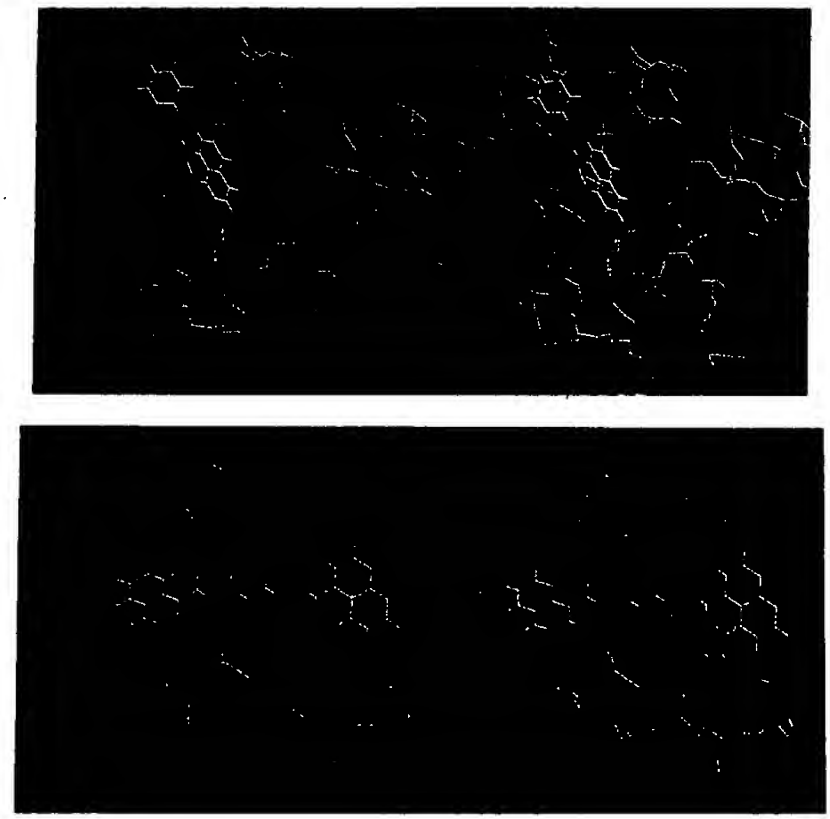

FIG. 4. (*Upper*) Stereo image of naphthol blue-black docked into the active site of cercarial elastase. (*Lower*) Stereo image of oxalic bis[(2-hydroxy-1-naphthylmethylene)hydrazide] docked into the active site of trophozoite cysteine protease. Catalytic residues are colored purple and labeled for orientation. The atoms on the inhibitors are color-coded: carbons are white, oxygens are red, nitrogens are blue, and sulfurs are cyan.

suggested by DOCK illustrate the challenges presented in accurately predicting the ligand–receptor complexes (43). For sulisobenzone, the failure to anticipate the binding of a counterion in the binding site led to an inaccurate prediction of the complex. In the case of phenolphthalein, a conformational change by an arginine between unbound and bound states of the enzyme and the presence of two waters in the bound state led to a slightly different conformation of the ligand than the one anticipated by DOCK (43). These examples highlight the importance of crystallography to the structure-based drug-design process. Ligand-induced conformational changes and the presence of bound waters and counterions are details that may be necessary for successful lead optimization.

The quality of the model structure is directly related to the percentage sequence identity between the relevant sequences. The trophozoite cysteine protease is ≈33% identical to both papain and actinidin, and the cercarial elastase is 20–25% identical to the seven mammalian serine proteases of known structure. Thus, we anticipate errors of 1–3 Å rms deviation in the model atomic coordinates, although errors in the vicinity of the active site are probably substantially smaller, reflecting selective sequence conservation. Two explanations of the success of our modeling/docking approach are plausible. (*i*) The modeling errors in the active site are small, and the major determinants of molecular recognition are faithfully recreated. (*ii*) Alternatively, the modeling process was irrelevant, and a homologous structure could have been substituted for computational ligand-binding studies to identify lead compounds. To address the latter possibility, two homologous serine proteases, chymotrypsin and trypsin, were used as receptors for ligand docking. Chymotrypsin was chosen because it shares with cercarial elastase a similar P1 specificity for hydrophobic residues. Trypsin was chosen because its S1 pocket is sterically similar, despite its different peptide specificity. With the same method, DOCK3.0 was used to search the Fine Chemicals Directory, and the top 2200 shape-complementarity scoring compounds and the top 2200 force-field scoring compounds were saved.

The best two inhibitors of the cercarial elastase were not included in either list of 4400 compounds predicted to inhibit chymotrypsin or trypsin, although each shape-based list included one of the less effective inhibitors. Due to unfavorable interactions seen in the model of 9-fluorenone-4-carboxylic acid docked to chymotrypsin (negative charge in hydrophobic S1 pocket), this compound would have been rejected during the visual-screening evaluation. Consequently, none of the five inhibitors identified for the cercarial elastase would have been found in a DOCK3.0 search by using the chymotrypsin active site, and only one of the 100 μM inhibitors, α-phenethylphthalamic acid, would have been found by using the trypsin active site. Although we cannot rule out finding other low-micromolar inhibitors from the lists of compounds generated by the chymotrypsin and trypsin searches, our results indicate that the modeling process was not irrelevant and that this method for inhibitor discovery is sensitive enough to differentiate between similar active sites in homologous structures.

Despite the inherent limitations of computer model-built structures, these structures are helpful in finding nonpeptidic inhibitors active at low-micromolar concentrations. Although these compounds are far from being drugs, they are sensible starting points for the process of drug development. Because these enzymes are members of two major protease families, our work suggests that computer models and structure-based drug-design methods can be applied to identify inhibitors of proteases that are relevant to other pathophysiologic processes.

We thank Elaine Meng and Cynthia Corwin for helpful suggestions and discussions and K. C. Lim for technical assistance. This work was supported by grants from the Defense Advanced Research Projects Agency (MDA-972-91-J1013 to F.E.C.) and the National Institutes of Health (GM07175 to C.S.R.; AI20452 to J.H.M.; F32AI08311 to E.S.; AI00870 to P.J.R.).

1. Stryer, L. (1988) *Biochemistry* (Freeman, New York).
2. Thomas, L., Leduc, R., Thorne, B. A., Smeekens, S. P., Steiner, D. F. & Thomas, G. (1991) *Proc. Natl. Acad. Sci. USA* **82**, 5297–5301.
3. Cohen, R. L., Xi, X. P., Crowley, C. W., Lucas, B. K., Levinson, A. D. & Shuman, M. A. (1991) *Blood* **72**, 479–487.
4. Navia, M. A. & Murcko, M. A. (1992) *Curr. Opin. Struct. Biol.* **2**, 202–210.
5. DesJarlais, R. L., Seibel, G. L., Kuntz, I. D., Furth, P. S., Alvarez, J. C., Ortiz de Montellano, P. R., DeCamp, D. L., Babe, L. M. & Craik, C. S. (1990) *Proc. Natl. Acad. Sci. USA* **87**, 6644–6648.
6. McKerrow, J. H. (1989) *Exp. Parasitol.* **68**, 111–115.
7. Read, R. J., Brayer, G. D., Jurasek, L. & James, M. N. G. (1984) *Biochemistry* **23**, 6570–6575.
8. Zuiderweg, E. R. P., Henkin, J., Mollison, K. W., Carter, G. W. & Greer, J. (1988) *Proteins* **3**, 139–145.
9. Weber, I. T. (1990) *Proteins* **7**, 172–184.
10. Chothia, C. & Lesk, A. M. (1986) *EMBO J.* **5**, 823–826.
11. Cohen, F. E., Gregoret, L. M., Amiri, P., Aldape, K., Railey, J. & McKerrow, J. H. (1991) *Biochemistry* **30**, 11221–11229.
12. Bruce-Chwatt, L. J. (1985) *Essential Malariology* (Wiley, New York).
13. Rosenthal, P. J., McKerrow, J. H., Aikawa, M., Nagasawa, H. & Leech, J. H. (1988) *J. Clin. Invest.* **82**, 1560–1566.
14. Rosenthal, P. J. & Nelson, R. G. (1992) *Mol. Biochem. Parasitol.* **51**, 143–152.
15. Rosenthal, P. J., McKerrow, J. H., Rasnick, D. & Leech, J. H. (1989) *Mol. Biochem. Parasitol.* **35**, 177–183.
16. Sutcliffe, M. J., Haneef, I., Carney, D. & Blundell, T. L. (1987) *Protein Eng.* **1**, 377–384.
17. Sutcliffe, M. J., Hayes, F. R. F. & Blundell, T. L. (1987) *Protein Eng.* **1**, 385–392.
18. Tsukada, H. & Blow, D. M. (1985) *J. Mol. Biol.* **184**, 703–711.
19. Meyer, E., Cole, G., Radhakrishnan, R. & Epp, O. (1988) *Acta Crystallogr.* **44**, 26–38.
20. Remington, S. J., Woodbury, R. G., Reynolds, R. A., Matthews, B. W. & Neurath, H. (1988) *Biochemistry* **27**, 8097–8105.
21. Navia, M. A., McKeever, B. M., Springer, J. P., Lin, T. Y., Williams, H. R., Fluder, E. M., Dorn, C. P. & Hoogsteen, K. (1989) *Proc. Natl. Acad. Sci. USA* **86**, 7–11.
22. Fujinaga, M. & James, M. N. G. (1987) *J. Mol. Biol.* **195**, 373–396.
23. Bode, W., Chen, Z., Bartels, K., Kutzbach, C., Schmidt, G. & Bartunik, H. (1983) *J. Mol. Biol.* **164**, 237–282.
24. Walter, J., Steigemann, W., Singh, T. P., Bartunik, H., Bode, W. & Huber, R. (1982) *Acta Crystallogr.* **38**, 1462–1472.
25. Greer, J. (1990) *Proteins* **7**, 317–334.
26. Kamphuis, I. G., Kalk, K. H., Swarte, M. B. A. & Drenth, J. (1984) *J. Mol. Biol.* **179**, 233–256.
27. Baker, E. N. & Dodson, E. J. (1980) *Acta Crystallogr.* **36**, 559–572.
28. Jones, T. A. & Thirup, S. (1986) *EMBO J.* **5**, 819–822.
29. Chothia, C. & Lesk, A. M. (1987) *J. Mol. Biol.* **196**, 901–917.
30. Singh, U. C., Weiner, P. K., Caldwell, J. W. & Kollman, P. A. (1986) AMBER (Dept. of Pharmaceutical Chemistry, Univ. of California, San Francisco), Version 3.0.
31. Gregoret, L. M. & Cohen, F. E. (1990) *J. Mol. Biol.* **211**, 959–974.
32. Luthy, R., Bowie, J. U. & Eisenberg, D. (1992) *Nature (London)* **356**, 83–85.
33. Chothia, C. (1976) *J. Mol. Biol.* **105**, 1–14.
34. Meng, E. C., Stoichet, B. M. & Kuntz, I. D. (1992) *J. Comp. Chem.* **13**, 505–524.
35. Rusinko, A., Sheriden, R. P., Nilakantan, R., Haraki, K. S., Bauman, N. & Venkataraghavan, R. (1989) *J. Chem. Inf. Comput. Sci.* **29**, 251–255.
36. Kuntz, I. D. (1992) *Science* **257**, 1078–1082.
37. Ferrin, T., Huang, C., Jarvis, L. & Langridge, R. (1988) *J. Mol. Graphics* **6**, 13–37.
38. McKerrow, J. H., Pino-Heiss, S., Lindquist, R. & Werb, Z. (1985) *J. Biol. Chem.* **260**, 3703–3707.
39. Grassetti, D. R. & Murray, J. F. (1967) *Arch. Biochem. Biophys.* **119**, 41–49.
40. Dixon, M. (1953) *Biochem. J.* **55**, 170–171.
41. Hanes, C. S. (1932) *Biochem. J.* **26**, 1406–1421.
42. Desjardins, R. E., Canfield, C. J., Haynes, J. D. & Chulay, J. D. (1979) *Antimicrob. Agents Chemother.* **16**, 710–718.
43. Shoichet, B. K., Stroud, R. M., Santi, D. V., Kuntz, I. D. & Perry, K. M. (1993) *Science*, in press.